Asian Journal of Geological Research

3(2): 42-54, 2020; Article no.AJOGER.57425

Modification of Zoeppritz Equations and Its Implications for Hydrocarbon Exploration: A Case Study of an Onshore Niger Delta Sedimentary Basin

Balogun Ayomide[1] and Adekunle Sofolabo[1*]

[1]Department of Physics/Geophysics, Geoscience Research Unit, University of Port Harcourt, Rivers State, Nigeria.

Authors' contributions

This work was carried out in collaboration between both authors. Author BA designed the study, wrote the protocol and wrote the first draft of the manuscript. Author AS performed the geophysical analysis of the study, managed the analyses of the study and the literature searches. Both authors read and approved the final manuscript.

Article Information

Editor(s):
(1) Dr. Ahmed Abdelraheem Frghaly, Sohag University, Egypt.
Reviewers:
(1) Abel G. Carrasquilla, Janeiro State University, Brazil.
(2) Hui Zhou, China University of Petroleum-Beijing, China.
(3) Edinei Koester, Universidade Federal do Rio Grande do Sul - UFRGS, Brasil.
Complete Peer review History: http://www.sdiarticle4.com/review-history/57425

Original Research Article

Received 29 March 2020
Accepted 05 June 2020
Published 22 June 2020

ABSTRACT

Zoeppritz equations are used to determine the reflection coefficient against the angle curves, which are often valid only for small seismic parameter changes across reflectors, but generally inaccurate close to the critical angle. These inaccuracies affect the quality of amplitude variations with offset (AVO) analysis, which might results in systematic errors when estimating relative seismic parameter variations at the reflectors. Thus modifying the Zoeppritz equations at the given angles allows for more accurate estimation of the usual AVO attributes, such as intercept, the gradient, and a possible third coefficient, which often leads to a better estimation of seismic-parameter contrasts at reflecting interfaces. The modification of Zoeppritz equations was analyzed using well data from oil fields in a sedimentary basin, onshore of Niger Delta area. This paper analyzed the modification of Zoeppritz equations and using them in AVO analysis to collect information on how seismic amplitudes vary with incident angles, which when combined with the P-P reflectivity (R_{PP}) or the P-S Reflectivity (R_{PS}) expressions, is used to obtain information on the properties of the

**Corresponding author: Email: adekunle.sofolabo@uniport.edu.ng;*

earth layers, with the emphasis only on interface reflectivity, while thin-bed effects, attenuation and other propagation factors well known to influence AVO measurements are not considered. The modified equations are subsequently used to generate the AVO reflectivity curves, the results obtained shows that the modified Zoeppritz predicted the AVO effects correctly for the different zones of interest in the basin. The results show that the Shuey's approximation gives better accurate results up to angle of 30^0 compared with others approximations, while the 3-term approximation shows that the modified Zoeppritz equations predicted AVO response accurately to about 50^0 of angle of incident. The result obtained can also be used to classify the different sand base types and their fluid contents, either oil, gas or brine sand base.

Keywords: Zoeppritz equations; reflectivity; amplitudes; offset; seismic waves; p-wave velocity; s-wave velocity.

1. INTRODUCTION

In seismology, Zoeppritz equations describe how seismic waves are transmitted and reflected at media boundaries between two different layers of earth. The solution of Zoeppritz equations [1,2] is given as the plane wave reflection and transmission coefficients as a function of the elastic parameters of both sides of the interface and the angles of incidence and transmission respectively. Zoeppritz equations are the basis of AVO (Amplitude Variations with Offset) or more properly AVA (Amplitude Variations with Angle) since the elastic parameters can be inferred from the amplitude variations with angle, which are commonly derived for the idealized situation of two half-spaces in a welded contact [3,4]. There are many forms of simplifications of the Zoeppritz equations of Primary-Primary (P-P) wave reflection coefficient, which each of these simplifications (in a degree angle) linked to the reflection amplitude with variations of the rock properties [5]. The Zoeppritz equation requires the continuity of displacement and stress (acceleration) at the interface, which results in a matrix equation for the amplitude of waves at any the given angle. The matrix coefficients depend on P-wave velocity, S-wave velocity and the density respectively, which are majorly dependent on the lithology, porosity, pore fluid content and temperature of the layer. There are different forms of scalar approximations to the matrix equations of the Zoeppritz published by different authors, which are usually based on the assumption of small incident angles [2,6,7].

1.1 Modification of Zoeppritz Equations

According to Bortfeld, the three terms reflectivity equation is a linearized form of the Zoeppritz equation, which predicts the amplitude (R) at various reflection angles (θ) given three reflectivity terms. These three terms are the zero-offset reflectivity (R_0), the P-wave reflectivity (R_p), and a gradient term (R_{sh}).

This is its basic form:

$$R(\theta_1) = R_0 + R_{sh}\sin^2(\theta) + R_p\tan^2(\theta_1)\sin^2(\theta_1) \quad (1)$$

Where,

$$R_P = \frac{\Delta V_P}{2V_P},$$

$$R_0 = R_P + R_\rho$$

$$R_\rho = \frac{\Delta \rho}{2\rho}$$

$$R_{sh} = \frac{1}{2}\left(\frac{\Delta V_p}{V_p} - k\frac{\Delta_p}{\rho} - 2k\frac{\Delta V_s}{V_s}\right) \quad (2)$$

$$k = \left(\frac{2V_s}{V_p}\right)$$

The linearized Bortfeld approximation allows us to invert seismic data to obtain the reflectivity of events. Unfortunately, most forms of the Bortfeld approximation involve the primary and shear wave interval velocities which are difficult to obtain without knowing the rock properties. While Aki and Richards, gave the Knot-Zoeppritz equations in a more convenient forms. These approximations are simpler and more practical than the original Zoeppritz equations, and for completeness, the reflection coefficients of the incident P-wave and reflected P-wave and S-wave are shown as follows:

$$PP = \frac{1}{2}\left(1 - 4\beta^2 p^2\right)\frac{\Delta\rho}{\rho} + \frac{1}{2\cos^2\theta}\frac{\Delta\alpha}{\alpha} - 4\beta^2\rho^2\frac{\Delta\beta}{\beta} \quad (3)$$

$$PS = \frac{-\rho\alpha}{2\cos\phi}\left[\left(1 - 2\beta^2 p^2 + 2\beta^2\frac{\cos\theta}{\alpha}\frac{\cos\phi}{\beta}\right)\frac{\Delta\rho}{\rho} - \left(4\beta^2 p^2 - 4\beta^2\frac{\cos\theta}{\alpha}\frac{\cos\phi}{\beta}\frac{\Delta\beta}{\beta}\right)\right] \quad (4)$$

$$R(\theta) = \left[\frac{1}{2}\left(1 + \tan^2\theta\right)\right]\frac{\Delta\alpha}{\alpha} - \left[4\frac{\beta^2}{\alpha^2}\sin^2\theta\right]\frac{\Delta\beta}{\beta} + \left[\frac{1}{2}\left(1 - 4\frac{\beta^2}{\alpha^2}\sin^2\theta\right)\right]\frac{\Delta\rho}{\rho} \quad (5)$$

The elastic properties in the above equations are related as follows to those on each side of the interface:

$$\Delta\alpha = \alpha_2 - \alpha_1,\ \alpha = \frac{\alpha_2 + \alpha_1}{2},$$

$$\Delta\beta = \beta_2 - \beta_1,\ \beta = \frac{\beta_2 + \beta_1}{2}, \text{ and} \quad (6)$$

$$\Delta\rho = \rho_2 - \rho_1,\ \rho = \frac{\rho_2 + \rho_1}{2}$$

The angle θ is the average of incident and transmitted P-wave angles while φ is the average of reflected and transmitted S-wave angle:

$$\theta = \left(\theta_2 - \theta_1\right) \text{ and } \phi = \frac{\phi_2 + \phi_1}{2} \quad (7)$$

Aki and Richards stated that primary reflectivity (R_{PP}) equation is rearranged in such a way that the influence of the offset or angle of incidence is separated [5]. Such that the first term influences the near traces (below 15 degrees), the second term starts its influence in the mid-range of incident angles (15-30 degrees), while the last term influences the large angles (above 30 degrees). The full three-term expression is equivalent to Aki and Richards, but the 2-term approximation is commonly used and is normally considered accurate up to an angle of about 30 degrees. This allows one to invert to only two variables, the two variables being combinations of the four Aki and Richards variables.

The result of these manipulations is given as:

The reflection coefficient equation is rearranged using Gelfands' method [8] after substituting for (Vp/Vs) = 2 as

$$R_{PP}(\theta) \approx \left[\frac{1}{4} - \left(\frac{V_S^2}{V_P^2}\sin^2\theta\right)\right]\left[\frac{\Delta V_P}{V_P} + \frac{\Delta\rho}{\rho}\right] + \frac{\Delta\alpha}{(1-\alpha)^2}\sin^2\theta + \frac{1}{2}\frac{\Delta V_P}{V_P}\left[\tan^2\theta - \frac{4V_S^2}{V_P^2}\sin^2\theta\right] \quad (8)$$

$$R_{PP}(\theta) \approx R_P + \left[A_0 R_P + \frac{\Delta\alpha}{(1-\alpha)^2}\right]\sin^2\theta + \frac{1}{2}\frac{\Delta V_P}{V_P}\left[\tan^2\theta - \sin^2\theta\right] \quad (9)$$

Where,

$$R_P = \frac{1}{2}\left(\frac{\Delta V_P}{V_P} + \frac{\Delta\rho}{\rho}\right) \quad (10)$$

$$G = A_0 R_P + \frac{\Delta\alpha}{(1-\alpha)^2} \quad (11)$$

$$A_0 = B - 2(1+B)\frac{1-2\alpha}{1-\alpha} \quad (12)$$

$$B = \frac{\Delta V_P / V_P}{\Delta V_P / V_P + \Delta\rho/\rho} \quad (13)$$

In this equation the first term represents the contribution of reflection coefficient at normal incidence commonly known as intercept, the second term represents the lithological component commonly known as gradient which becomes more prominent with offset and third term becomes significant at a larger angle of incidence. For angle of incidence between 0 - 30 degree, the value of tan and sin will be approximately the same therefore; the contribution of this term becomes insignificant.

Thus, ignoring the third term, equation (9) can be rewritten as

$$R_{PP}(\theta) \approx R_P + G\sin^2\theta \quad (14)$$

Where G is the gradient term and depends on V_p/V_s ratio.

i.e. $$G = \left(\frac{1}{2}\right)\left[\left(\frac{\Delta V_P}{V_P}\right) - \left(\frac{\Delta\rho}{\rho}\right) - 2\left(\frac{\Delta V_S}{V_S}\right)\right]$$

Equation (14) represents a simple straight line equation which provides Rp as intercept and G as slope (or gradient), if R (θ) is plotted against $\sin^2\theta$. In deriving the above expression of P-wave reflection coefficient R_{PP} (θ) given in equation (14), the following assumptions were made:

- The medium of seismic wave propagation is isotropic and homogeneous.
- The values Δρ, ΔVp and ΔVs are small compared to ρ, Vp and Vs.
- Angle of incidence is less than the critical angle.
- Shear wave velocity is assumed half of the P-wave velocity i.e., (Vp/Vs) = 2.
- For angle of incidence range 0 to 30 degree, the value of tan θ and sin θ will be approximately same, therefore; the contribution of third term in P-wave reflection coefficient equation (9) becomes insignificant and hence ignored for all practical purposes.

In the case of R_{PS} one obtains an odd-power series of sine functions and R_{PS} is sometimes approximated as a function linear in the sine. Ramos and Castagna [9] obtained the expression appropriate to R_{PS}. The goal of this paper is to use a good log data to analyze the modified Zoeppritz equation, using them in AVO analysis to collect information on how seismic amplitudes vary with incident angle, and to use this along with R_{PP} (or R_{PS}) expressions to obtain information on properties of earth layers. This exact and modified equation will be used to generate AVO reflectivity curves of the data from Niger- Delta.

2. MATERIALS AND METHODS

2.1 Materials

2.1.1 Data presentation

Well data from Shell Producing Development Commission (SPDC) and software (RokDoc 5.0 from Ikon Science and CREWES Reflectivity Explorer 2.0) was used for the analysis. The depth type used is the True Vertical Depth (TVD) below the Kelly Bushing (TVD*kb*), which is equal to the True Vertical Depth given for un-deviated well in the data.

$$KB = \text{TVD}kb - \text{TVD}ss$$

The well KB used is 56.66ft, where KB is the well Kelly Bushing and TVDss is the true vertical depth below sea level.

2.2 Methods

2.2.1 Single interface modeling

The exact and modified Zoeppritz equations are used to generate AVO reflectivity curves for a single interface, separating two isotropic materials, assuming an incident plane wave. These assumptions are potentially problematic and can lead to erroneous conclusions. If one of the layers is anisotropic, then a modified form of the Zoeppritz equations must be used. Note that isotropy implies that the seismic velocity is the same in all directions, whereas anisotropy implies that that the velocity changes as a function of direction [1,4,10].

3. RESULTS AND DISCUSSION

3.1 Reflectivity Cross-Plots

The cross plots of the brine sand overlying shale reflection for both exact P-P and P-S reflection coefficient as a function of incident angle (Fig. 1). The P-S reflection coefficient is zero at normal incidence, which increases to a peak at an intermediate angle of incidence, and then drops in amplitude at larger angles of incidence. The P-P reflection coefficient increases in magnitude with the incident angle and is bigger than the magnitude of P-S reflection coefficient.

The graph has a trend in which the reflectivity increases with a corresponding θ value. It gradually increases in reflectivity from 0.3-0.5 also with a sharp increase in the incident angle from 0^0 -50^0. Both the near and far offset is located on the zero value of the reflectivity and on 10^0 and 30^0 respectively on the incident angle value.

The earth properties used for this graph are:

- **P-wave velocities (Vp):** In brine sand is 3271.484 ms^{-1}, and in shale 3190.554 ms^{-1}.
- **S-wave velocities (Vs):** In brine sand is 1772.898 ms^{-1}, and in shale 1590.269 ms^{-1}.
- **Densities (ρ):** In brine sand 2.228 gcm^{-3}, and in shale 2.439 gcm^{-3}.

Using a Poisson ratio of 0.292 for the brine sand layer and 0.335 for the shale layer, the Figure shows the magnitude of the reflection coefficients increasing with increasing angle of incident and this can be classified as a Class FC (fluid contact) AVO. This is also a case of Class -3 AVO, characterized by peak increase in amplitude with offset i.e. increasing positive amplitude with increasing offset [11].

3.2 Cross-plots of Modification of Zoeppritz Equations

The cross plot of the modification of the Zoeppritz equations (Fig. 2) shows the four modifications for P-P reflection coefficient of the exact equation using Shuey's approximation, which is valid for angles of incidence up to 30°–35°. This assumption is made such that the value of V_P is approximately twice that of V_S, while higher terms are dropped under the 30° angle-of-incidence condition. The P-S reflection coefficient of the modified equations at normal incidence to the interface is assumed to be zero, which increase slightly on the positive reflection coefficient before it becomes negative immediately after the far offset angle i.e. 30° (Fig. 3). This occurs for only Zoeppritz and its approximation except for Shuey's approximation, which shows a slight increase. Aki and Richards' approximation of P-S reflectivity can be regarded as good for small incident angles and small S-wave property changes. It shows more accuracy at far offset compared to Shuey's approximation, while Bortfeld's P-S approximation cannot be performed on the version of the software. We also observed on the software that all the three-term approximations show almost the same trend in both P-P and P-S approximations expect for Bortfeld's P-S approximation. The combination of the P-P and P-S reflectivity on the same plot with different ranges of the incident angles is shown in Fig. 4, which shows a clear comparison of the exact and modified equation for both P-P and P-S at angle 0°-50° and 0°-90° respectively. The angle at which the magnitude of classified sand reflection coefficient decreases with increasing angle of the incident was observed. The reflection decreases at 50° for P-P reflectivity and at 30° for P-S reflectivity.

3.3 Multiple Interfaces Cross-Plots

The assumption that there is only one layer is wrong but can be a useful approximation. When multiple interfaces and layers are included in the model, factors that influence the amplitude such as multiples, converted waves, transmission losses(not treated in this paper) all occur. Since these are not included in our simplistic AVO model, they must be appropriately processed so as not to influence the estimates of the elastic parameters. Showing below are reflection coefficients for the three-layer gas sand model. Three-layered model of sand-shale-sand formation has shale with Poisson's ratio of 0.336, embedded between a gas sand layer with a Poisson's ratio of 0.314 and a brine sand layer with a Poisson's ratio of 0.316 (Fig. 5). The earth properties used for this graph are:

- **P-wave velocities (Vp):** In gas sand is 3179.315 ms^{-1}, in brine sand 3165.612 ms^{-1}, and in shale 3110.327 ms^{-1}.
- **S-wave velocities (Vs):** In gas sand is 1654.51 ms^{-1}, in brine sand 1641.38 ms^{-1}, and in shale 1545.879 ms^{-1}.
- **Densities (ρ):** In gas sand is 2.244 gcm^{-3}, in brine sand 2.170 gcm^{-3} and in shale 2.147 gcm^{-3}.

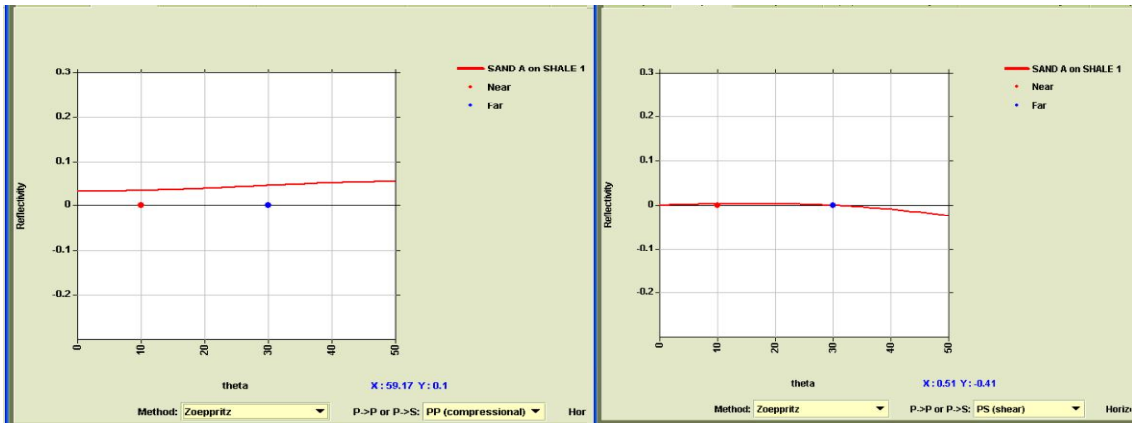

Fig. 1. SAND A on SHALE 1, brine sand over shale reflection for Exact P-P and P-S reflection coefficient as a function of incident angle. The magnitude of Class FC sand reflection coefficients decreases with increasing angle of incidence

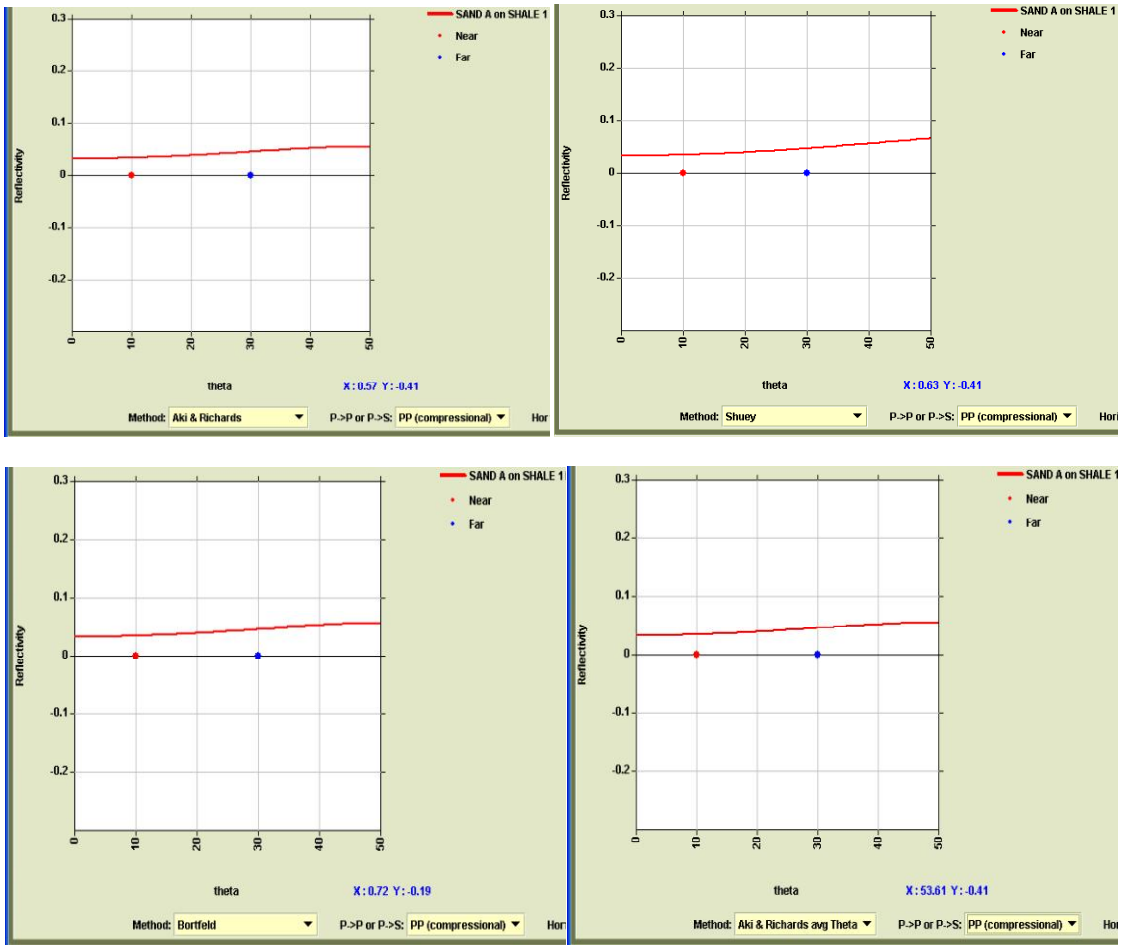

Fig. 2. SAND A on SHALE 1, brine sand over shale reflection for Modified P-P reflection coefficient as a function of incident angle. The magnitude of Class FC sand reflection coefficients decreases with increasing angle of incidence

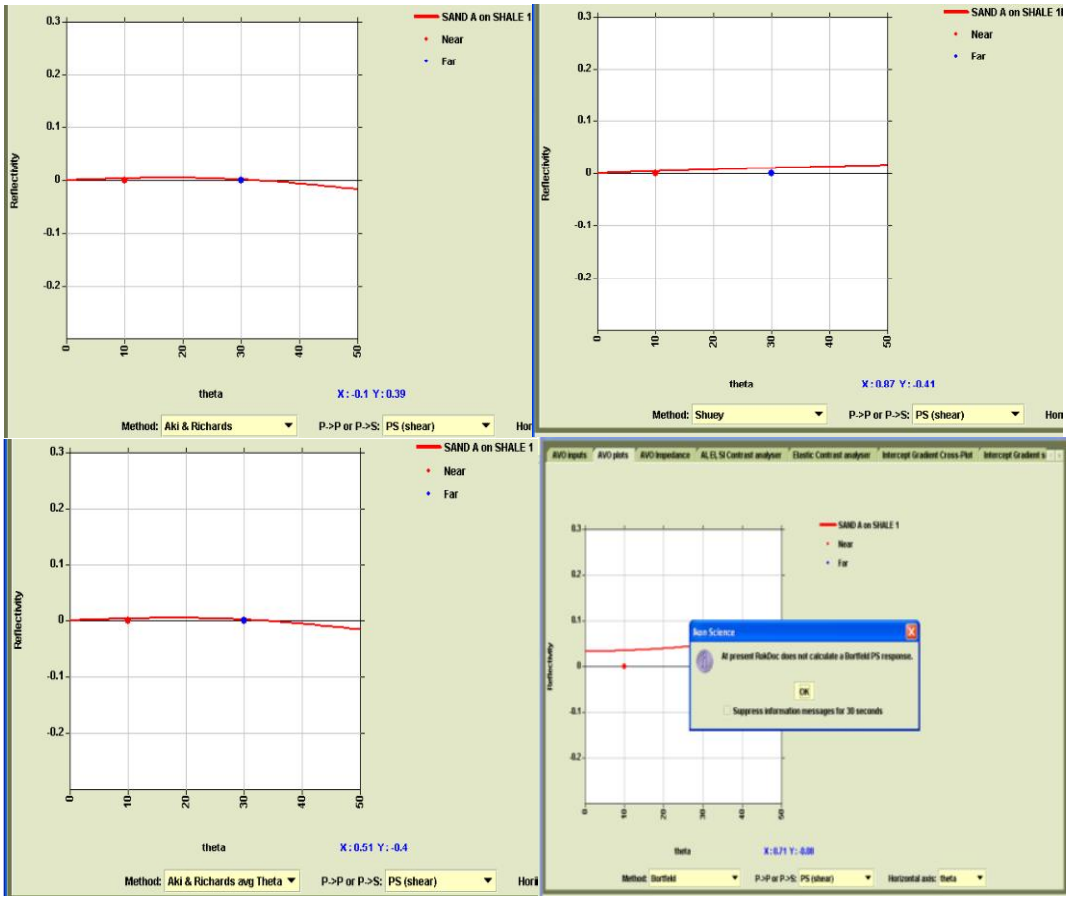

Fig. 3. Modified P-S reflection coefficient of SAND A (brine sand) over SHALE 1. The magnitude of Class FC sand reflection coefficients decreases with increasing angle of incidence

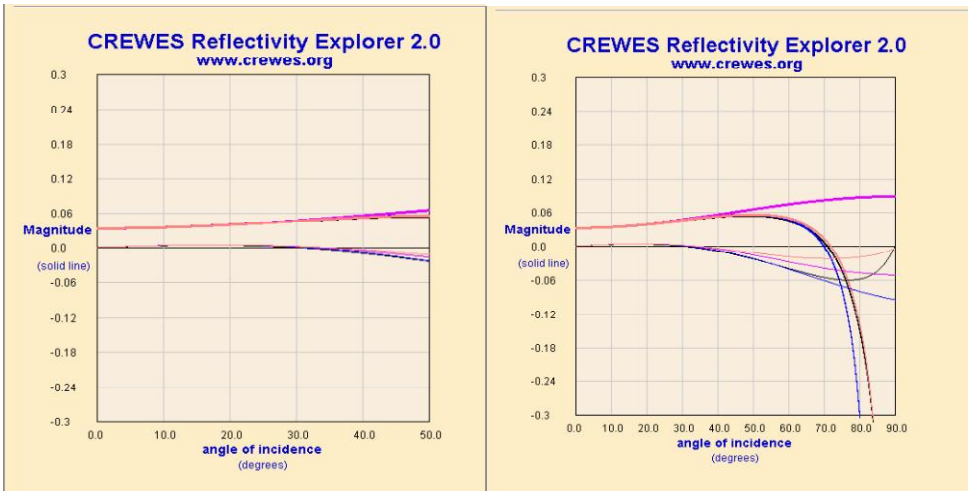

Fig. 4. A clear comparison of the exact and modified equation for both P-P and P-S Reflectivity of the (brine sand) SAND A overlying SHALE 1 for a range of incidence angles from 0^0 to 50^0 and from 0^0 to 90^0. Where the colour codes are: Exact Zoeppritz (black), Bortfeld (salmon), Aki-Richard (blue) and Shuey 2-term (magenta)

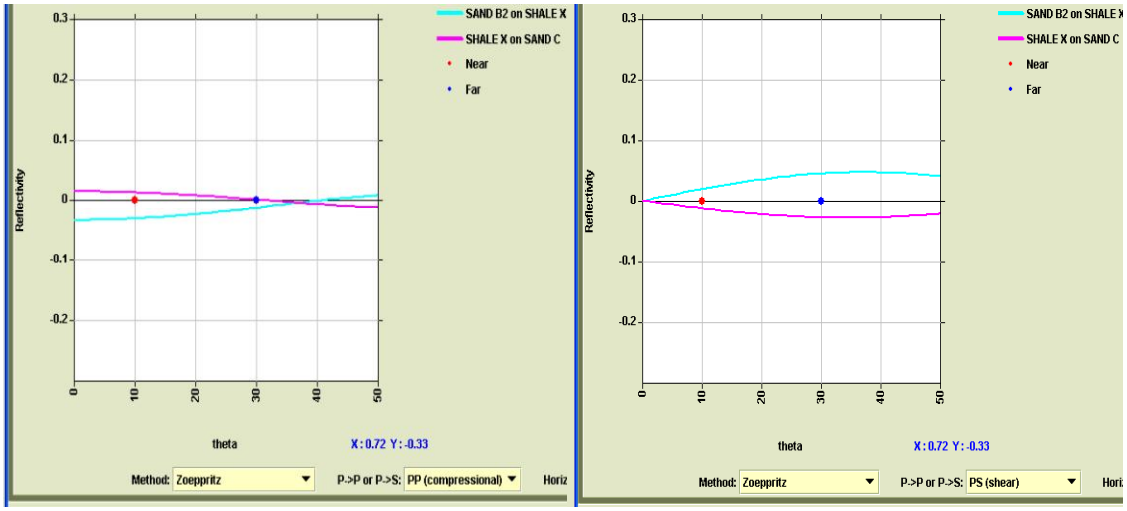

Fig. 5. Exact P-P and P-S Reflectivity of Gas sand over shale (SAND B2 on SHALE X, reflection coefficient decreases with increasing offset) and shale over brine-sand (SHALE X on SAND C, decrease in amplitude versus offset) reflections

The first formation is Sand B2 on Shale X, which is gas sand over shale formation with Sand B2 having a lower relative impedance. The exact P-P and P-S reflectivity of a Class IV AVO, where the reflection coefficient decreases with increasing offset is shown in Fig. 5. A Class IV AVO response (lower-impedance gas sands) has a trough that dims with offset and they are anomalous in that they have a positive AVO gradient.

The second interface which is the Shale X over Sand C, which is shale over brine sand formation, is a Class I AVO. Class 1 AVO response (higher-impedance sand) has a peak at zero-offset that deceases with offset and changes polarity at far offset. The normal incidence reflection coefficient is positive while the AVO gradient is negative and the reflection coefficient decreases with increasing offset. For the exact P-S reflectivity, the trend started from zero then gradually increased to a peck 38° and dropped gradually (Fig. 6) but for Shuey's approximation, there was a sharp increase (Fig. 7) while other approximation dropped gradually. Fig. 6, shows the modified P-P reflectivity, with Shuey's approximation, valid for angles of incidence up to 30°–35°.

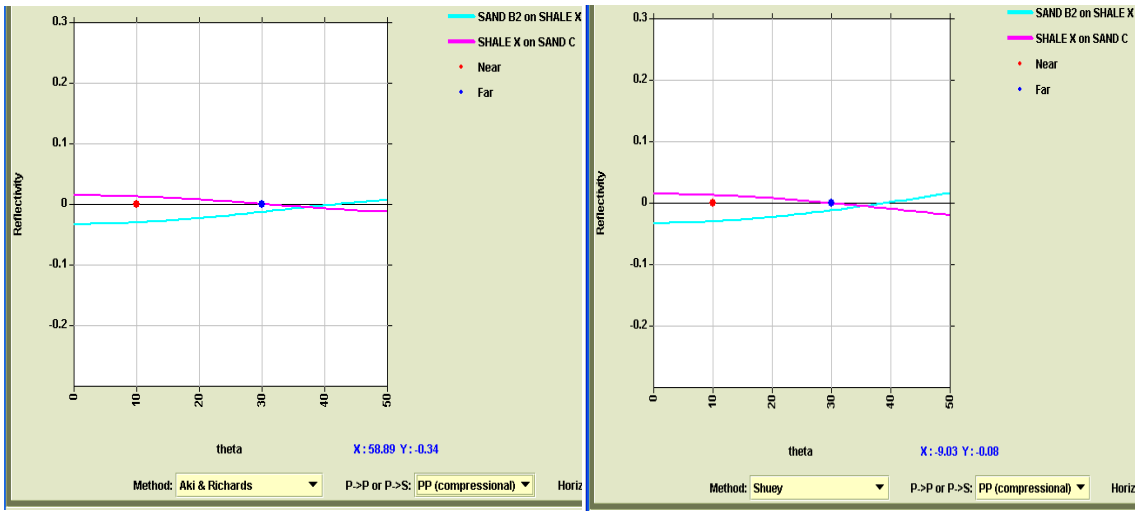

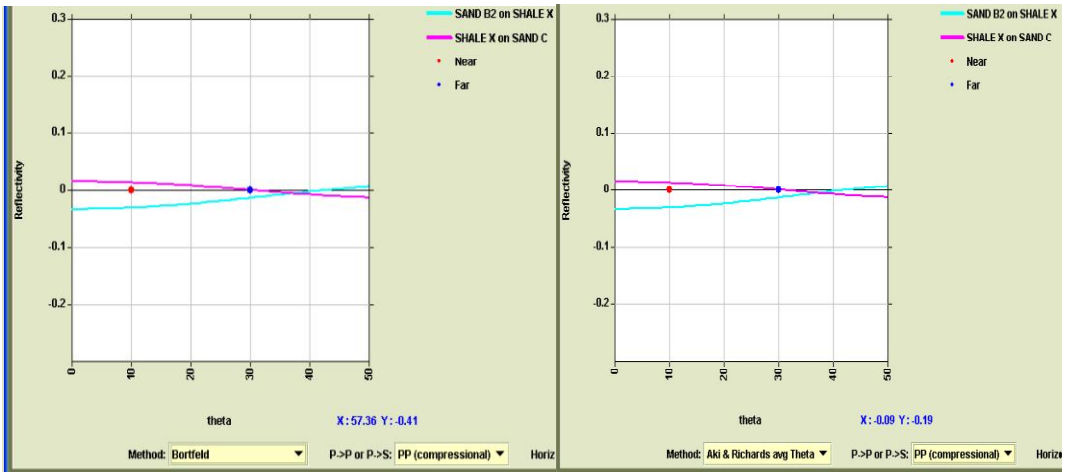

Fig. 6. Modified P-P Reflectivity of Gas sand over shale (SAND B2 on SHALE X, reflection coefficient decreases with increasing offset) and shale over brine-sand (SHALE X on SAND C, decrease in amplitude versus offset) reflections

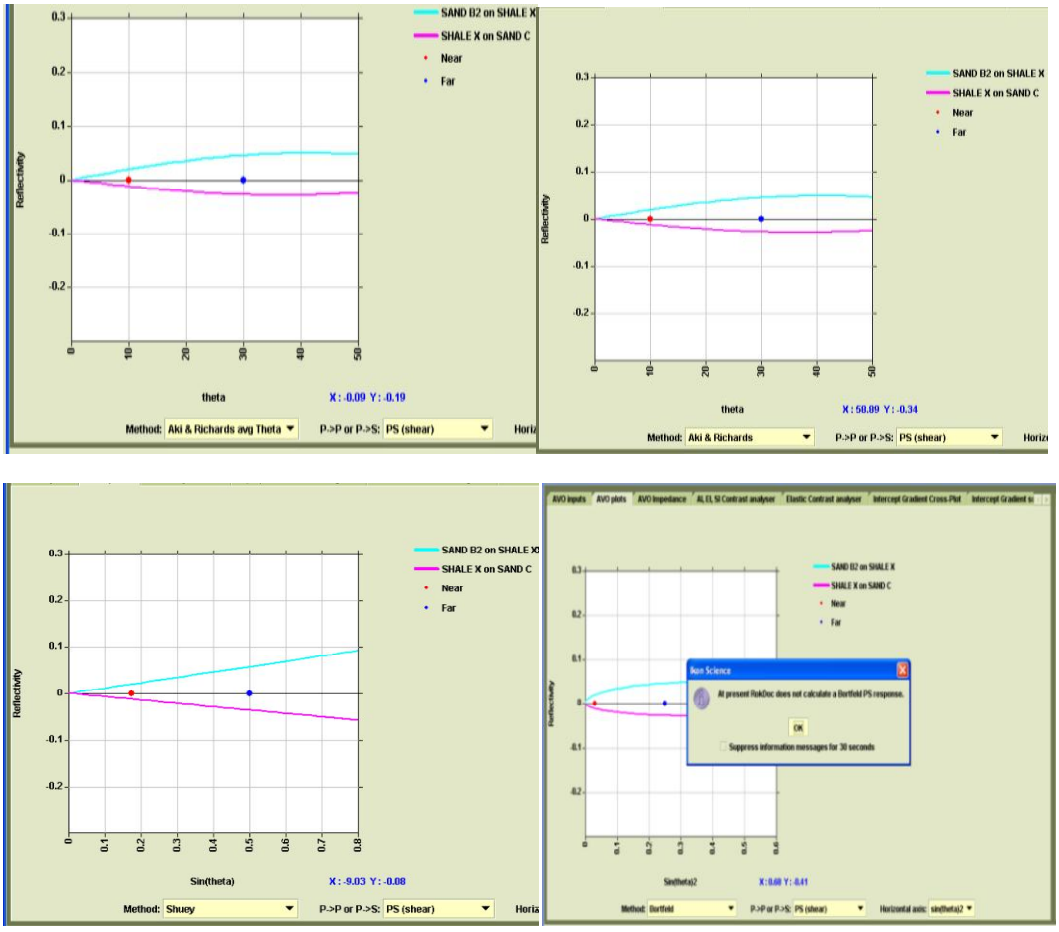

Fig. 7. Exact and Modified P-S Reflectivity of Gas sand over shale (SAND B2 on SHALE X, reflection coefficient decreases with increasing offset) and shale over brine-sand (SHALE X on SAND C, decrease in amplitude versus offset) reflections

The combination of the exact and modified (maintain their colour-codes from previous Figures) P-P and P-S reflectivity on the same plot with different ranges of the incident angles are shown in Fig. 8, with incident angle ranging from 0° - 50° for both Sand B2 on Shale X and Shale X on Sand C, while Fig. 9 shows the incident angle from 50° to 90° for both Sand B2 on Shale X and Shale X on Sand C respectively. The result obtained clearly shown a clear comparison of the exact and modified equation for both P-P and P-S at incidence angle between 0°-50°, with a critical angle at 79.28° (Fig. 8), showing that the velocities of the Shale X is greater than that of Sand C. There was a phase change for exact and modified P-S reflectivity except for Shuey's approximation.

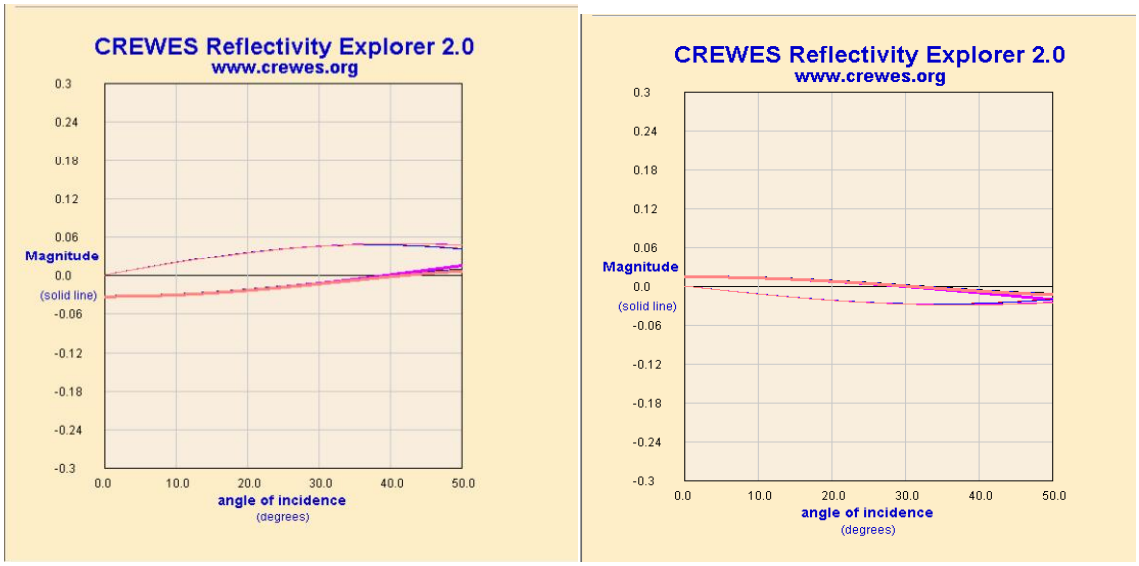

Fig. 8. A clear comparison of exact and modified equation of both P-P and P-S Reflectivity of SAND B2 (gas sand) overlying SHALE X and SHALE X overlying SAND C for a range of incidence angles from 0^0 to 50^0. Where the colour codes are: Exact Zoeppritz (black), Bortfeld (salmon), Aki-Richard (blue) and Shuey 2-term (magenta)

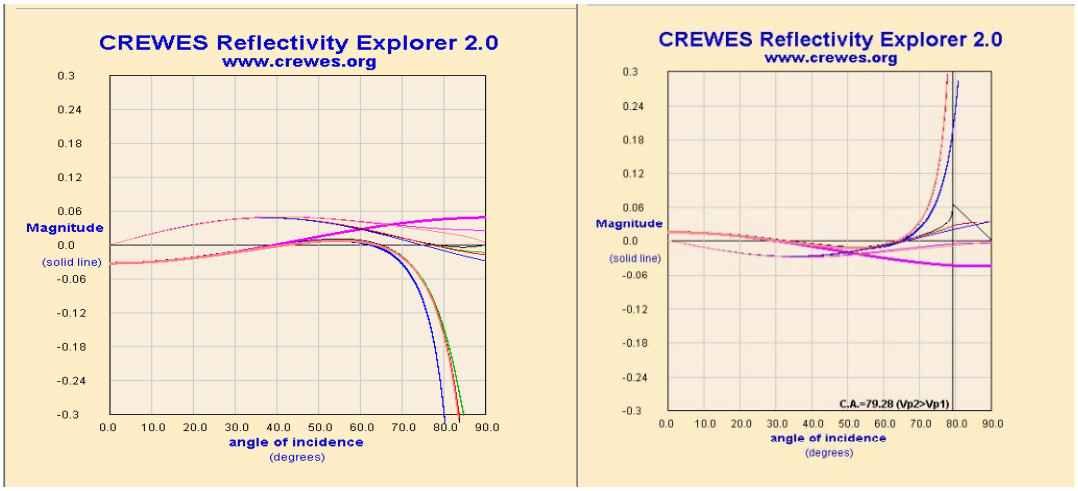

Fig. 9. A clear comparison of the exact and modified equation of both P-P and P-S Reflectivity of SAND B2 overlying SHALE X and SHALE X overlying SAND C for a range of incidence angles from 0^0 to 90^0. Where the colour codes are: Exact Zoeppritz (black), Bortfeld (salmon), Aki-Richard (blue) and Shuey 2-term (magenta)

Table 1. Fluid type in reservoirs with the density and Poisson ratio values

Properties	Density (g/cm^3)	Poisson Ratio	Fluid Type
Sand A	2.228	0.292	Brine sand
Sand B	2.226	0.318	Probable Oil sand
Sand B2	2.244	0.314	Gas sand
Sand C	2.170	0.316	Gas sand

Table 2. Sand Interface - Intercepts, gradients and Classes of AVO responses

Interface	Intercepts(I)	Gradient (G)	AVO Classification
Sand A on Shale 1	0.035	0.05	FC
Sand B2 on Shale X	-0.034	0.076	IV
Shale X on Sand C	0.016	-0.058	I
Shale B on Shale Y	-0.014	0.018	IV

At the critical angle, the partitioning of energy changes radically. At the angle of incidence less than critical angle, some of the incident energy is transmitted as compressional energy and maybe further partitioned at the next interface. At incident angle greater than critical angle, no compressional energy is transmitted and as a result, seismic reflection method fails. At critical angle, there is no reflection of shear waves but minor shear energy is transmitted. With further increase in angle of incidence, the shear energy reflection and transmission becomes maxima and then it starts decreasing with a further increase of angle of incidence. The maximum value of shear wave reflection and transmission depends on (V_p/V_s) ratio.

The results obtained are summarized in Table 1, showing the fluid types in the reservoir that was investigated with their corresponding density and Poisson's ratio, while Table 2 gives the interface intercept and gradient with the classes of AVO.

4. CONCLUSION

Based on the results obtained from the research of modification of Zoeppritz equations, we can conclude that:

- Aki and Richard approximation gives reliable reflectivity compares to the full Zoeppritz equations.
- Shuey's two-term approximation is more effective than the other approximations and it is valid for angle of incidence up to 30^0 - 35^0.
- There are three different types of sand based on their fluid contents, namely: Oil sand, Gas sand and Brine sand respectively.
- A probable Oil sand falls under four classes of AVO response, classes I, II, IV, and FC. While the gas and brine sand falls under class FC and class I & IV respectively.
- Each AVO response lies on a similar trend but with a different offset.
- The variation in trend is due to changes in fluid content and rock properties.
- Hydrocarbon filled sandstone reservoirs display higher reflectivity than water wet reservoir.

5. RECOMMENDATION

From the results of the research, we observed that clean brine sand can appear more anomalous than less porous hydrocarbon-bearing sand. This implies that no matter what tools are used for AVO interpretation, there is still potential for ambiguity and therefore AVO studies should not be used in isolation. Though progress has been made in modeling, processing and interpretation, AVO can still be improved on by joint effort from the seismic, logging and Petrophysics communities.

CONSENT

All authors declare that written informed consent and approval was obtained from all concerned parties and company for the publication of information and images used in this research. A copy of the written consent is available for review by the Editorial office/Chief Editor/Editorial Board members of this journal.

ACKNOWLEDGEMENTS

The research team wishes to thank the Geophysics research unit of the University of Port Harcourt and Shell Petroleum Development Company (SPDC), for permission to use the information and images for this study.

COMPETING INTERESTS

Authors have declared that no competing interests exist.

REFERENCES

1. Zoeppritz K. Erdbebenwellen VIIIB, on the reflection and propagation of seismic waves: Göttinger Nachrichten. 1919;I:66-84.
2. Aki KI, Richards PG. Quantitative seismology - Theory and methods, volume I, sec. 5.2: W. H. Freeman and Company, San Francisco; 1980.
3. Yong Xu. Rock physics and seismic methods for characterizing the heterogeneity of oil sands reservoirs in the Western Canadian Sedimentary Basin. PhD Thesis; 2012.
4. Balogun A, Ebeniro JO. Evaluation of seismic attributes generated from extended elastic impedance for lithology and fluid discrimination, International Journal of Science and Research (IJSR). 2017;6(9):776–779.
5. Shuey RT. A simplification of the Zoeppritz Equations: Geophysics. 1985;50:609-614.
6. Balogun A, Ehirim CN. Lithology and fluid discrimination using bulk modulus and mu-rho attributes generated from extended elastic impedance, International Journal of Science and Research (IJSR). 2017;6(10): 639 – 643.
7. Bortfeld R. Approximations to the reflection and transmission coefficients of plane longitudinal and transverse waves: Geophysical Prospecting. 1961;9:485-502.
8. Gelfands VP, Nguyen H, Larner K. Seismic lithology modeling of amplitude verses offset data, 56th Annual meeting and international exposition, Society Exploration. Geophysics, Expanded abstracts. 1986;334-337.
9. Ramos ACB, Castagna JP. Useful approximations for converted-wave AVO: Geophysics. 2001;66:1721-1734.
10. Awosemo OO. 'Evaluation of Elastic Impedance Attributes in Offshore High Island, Gulf of Mexico', (MSc. Thesis), Department of Earth and Atmospheric Sciences, University of Houston. USA; 2012.
11. Young RA, LoPiccolo RD. A Comprehensive AVO Classification: The Leading Edge. 2003;11-18.

APPENDIX

Geophysical Logs Plots Showing Different Working Interval

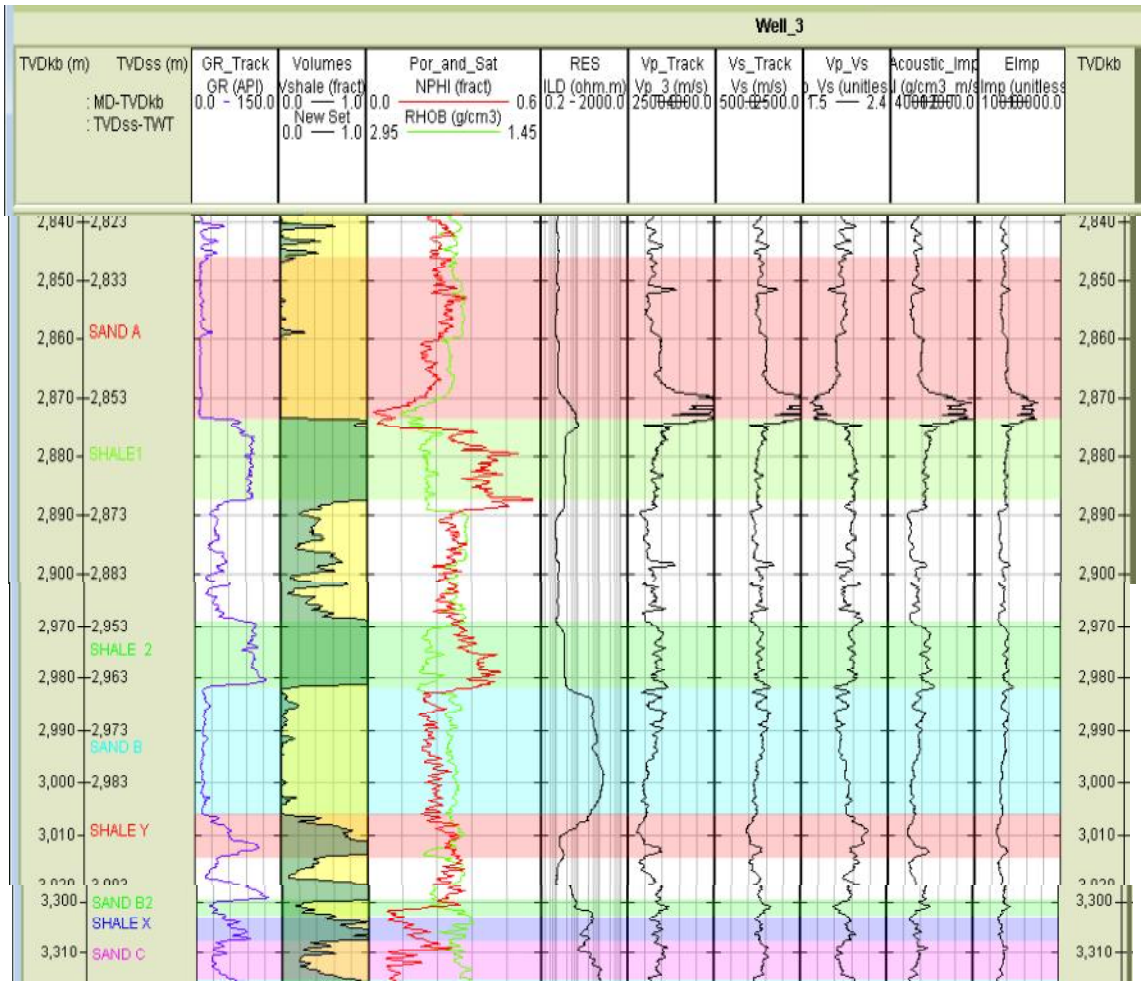

A Geophysical logs showing SAND A, SHALE 1, SHALE 2, SAND B, SHALE Y, SAND B2, SHALE X, and SAND C, at different sand interval. The appendix shows the depth plots of logs. Track 1 represents the Gamma ray (API) and Caliper (inch) logs. Track 2 is the Shale volume log, track 3 is the Neutron Porosity (NPHI in fraction) and Bulk density (RHOB in g/cc) plots with depth. Track 4 is the Resistivity log measured with deep Induction log (ILD) in ohms-meter. Track 5 ,track 6 ,track 7,Track 8 and Track 9 represent the V_P (m/s), V_S(m/s), V_P/V_S ratio, acoustic impedance and elastic impedance respectively. Using the gamma-ray log, shale volume log, resistivity log, neutron porosity and density logs, different lithologies were identified.

© 2020 Ayomide and Sofolabo; This is an Open Access article distributed under the terms of the Creative Commons Attribution License (http://creativecommons.org/licenses/by/4.0), which permits unrestricted use, distribution, and reproduction in any medium, provided the original work is properly cited.

Peer-review history:
The peer review history for this paper can be accessed here:
http://www.sdiarticle4.com/review-history/57425